Micro Materials
Excellence in Nanomechanics

Updated for 2024

NanoTest High Temperature Publications

Introduction

Material properties can vary greatly with changes in temperature. Thus, when developing or characterising the mechanical properties of coatings and bulk materials for high temperature applications, test conditions should mimic in-service conditions as closely as possible.

Nanomechanical tests have been performed with Micro Materials NanoTest systems at test temperatures up to 1000 °C. This has led to a number of publications on a wide range of materials.

In the tables on pages 2-5 of this note, published NanoTest studies are grouped into several categories based on the material tested:

(1) Nuclear materials
(2) PVD coatings for cutting tools
(3) Aerospace materials
(4) Materials with other high temperature applications

The maximum test temperature and year of publication is shown for each reference. The choice of indenter material and test environment is influenced by the sample being tested and the test temperature range. These factors are discussed in detail in *Nanomechanics to 1000 °C for high temperature mechanical properties of bulk materials and hard coatings* [ref 48].

The figure below shows the maximum published nanomechanical testing temperatures for various nanoindenter system configurations up to 2019. The dominance of the NanoTest (+) is demonstrated, in particular for temperatures > 500 °C.

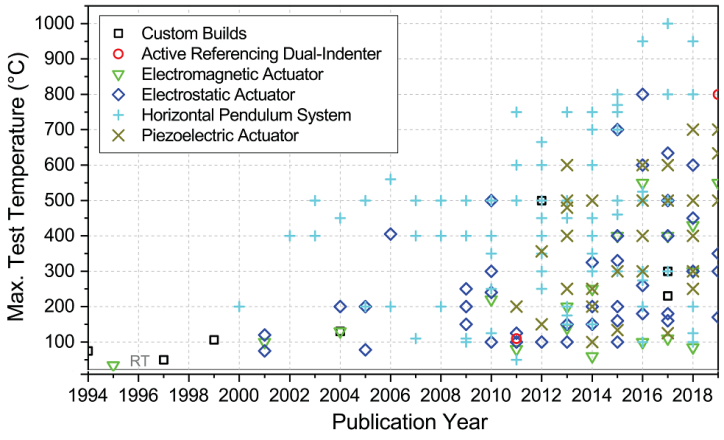

Important factors for High Temperature Testing

When measuring at elevated temperatures, it is essential that the sample and indenter are the same temperature when the indentation takes place. Any temperature mismatch will result in higher thermal drift, i.e. measurement error, caused by an expansion or contraction of the sample, indenter or instrument.

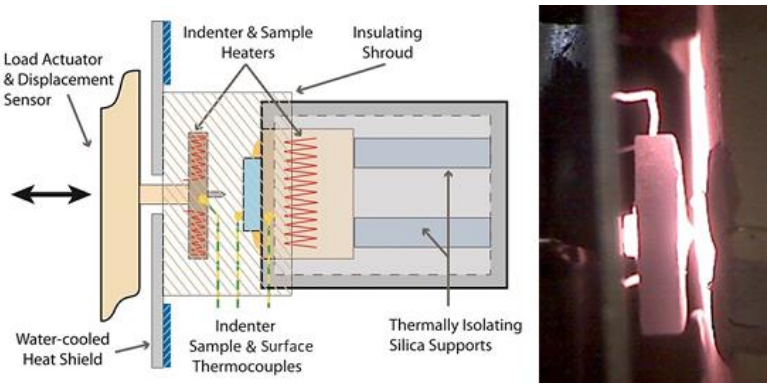

The horizontal high temperature configuration of the NanoTest (left) and a close-up view of an indenter and sample at 950 °C in vacuum (right). (Figures above left and below left courtesy of Dr Jeff Wheeler, ETH Zurich.)

NanoTest systems have design advantages which result in ultra-low thermal drift up to the maximum temperatures of 850 °C for the Vantage system, and 1000 °C for the NanoTest Xtreme:

Active tip heating – the indenter and the sample are both actively and independently heated, resulting in an isothermal contact *before* the experiment begins.

Horizontal loading – the unique load head configuration of the NanoTest systems means that there is no heat flow onto the loading head or depth measurement sensor.

Highly localised heating – a heat shield and insulating shroud around the heated zone ensures instrument stability during high temperature experiments.

Patented control protocol – software routines are used to precisely match the indenter and stage temperatures to ±0.1 °C.

Time-dependent measurements – As no significant thermal drift occurs during high temperature measurements it becomes possible to perform long duration tests such as indentation creep tests and SPM imaging.

1. Nuclear materials

Materials System	Indenter material	Test environment	Max. test temp. (°C)	Year	Reference
304 austenitic stainless steel	cBN	argon	300	2015	1
Zr-2.5%Nb	sapphire	air	400	2011	2
Nanoscale metallic multilayers	diamond	argon	400	2013, 2014, 2018	3-6
SiC in TRISO fuel particles	diamond	air	500	2015, 2016	7, 8
SiC-SiC composite	cBN	95%Ar/5%H_2	500	2019	9
PM2000 ODS alloy	cBN	argon	600	2014	10
PH 13-8 Maraging steel	cBN	95%Ar/5%H_2	625	2016	11
W-1%Ta alloy	cBN	vacuum	700	2020	12
Tungsten	cBN	vacuum	750	2015	13
Inconel 617	cBN	air	800	2017	14
Tungsten	cBN	vacuum	950	2015, 2017, 2018	15-17
Pyrolytic graphite	diamond	vacuum	600	2022	50
δ-phase zircaloy hydride	diamond	nitrogen	300	2020	51
Inconel 718	cBN	nitrogen	650	2019	54
Uranium dioxide	cBN	argon	500	2021	55
Uranium dioxide	cBN	argon	600	2019	56
ODS steels	cBN	argon	600	2019	61
Inconel 625/BNi-2	diamond	air	490	2020	69
Inconel 617	diamond	air	200	2016, 2018	72, 73
Tungsten carbide	diamond	vacuum	600	2023	75

2. PVD hard coatings

Materials System	Indenter material	Test environment	Max. test temp. (°C)	Year	Reference
TiAlN and TiN	diamond	air	300	2019	18
TiAlN	diamond	air	350	2012	19
TiAlN, AlCrN	diamond	air	500	2006	20
AlTiN	diamond	air	500	2006, 2008	21-23
TiAlN	diamond	air	500	2007	24
TiAlCrSiYN/TiAlCrN	cBN	argon	600	2012	25, 26
TiAlSiN	cBN	argon	600	2019	27
SiC, SiCN	cBN	argon	650	2015	28
TiAlN, TiCN	cBN	argon	750	2014	29
Ti_2AlN MAX phase	sapphire	vacuum	800	2022	62
DLC coatings	diamond	air	400	2020	66
Al/SiC nanolaminates	diamond	air	150	2020	67
TiN/ZrN nanolaminates	cBN	argon	450	2023	70
Nanolayered CrAlTiN	cBN	argon	700	2014	71

3. Aerospace materials

Materials System	Indenter material	Test environment	Max. test temp. (°C)	Year	Reference
Ni-base superalloys	sapphire	argon	400	2008	32, 33
Ni-base superalloy	sapphire	vacuum	665	2012	34
Ni-base superalloy, MCrAlY bond coat	sapphire	vacuum	1000	2017	35
SiC ceramic matrix composites	sapphire	argon	800	2021	49

4. Other materials

Materials System	Indenter material	Test environment	Max. test temp. (°C)	Year	Reference
(Pr,Ce)$O_{2-\delta}$ cathode material	cBN	argon/N_2	600	2016	30
G18 glass-ceramic	cBN	argon	750	2011	31
δ-$Mg_{17}Al_{12}$ phase	sapphire	air	278	2016	36
Magnesium	diamond	air	300	2015	37
NiTiHf shape memory alloy	diamond	air	340	2017	38
$MgAl_2O_4$ spinel	diamond	air	400	2009	39
Silicon (100)	diamond	air	400	2009	40
AlCu alloy	cBN	argon	460	2016	41
CuNb composite	cBN	argon	500	2015	42
Fused silica	cBN	argon	600	2011	43
Gold	sapphire	vacuum	665	2012	34
CVD Al_2O_3 coating	cBN	95%Ar/5%H_2	700	2015	44
WC-Co	cBN	vacuum	700	2020	45
Silicon	cBN	vacuum	770	2017	46
Cr_2AlC MAX-phase	sapphire	vacuum	980	2019	47
Ti-based bulk metallic glasses	diamond	argon	400	2020	52
Bulk metallic glasses	diamond	air	200	2020	53
Sintered nano-copper	diamond	air	200	2022	57
magnesium/carbon nanotube nanocomposites	cBN	argon	300	2021	58

Materials System	Indenter material	Test environment	Max. test temp. (°C)	Year	Reference
SiC/Al–Cu nanocomposites	diamond	air	300	2022	59
MgCoNiCuZnO Entropy stabilized oxide	cBN	air	950	2022	60
Al/SiC Composites	diamond	air	500	2002	63
Fe-based metallic glass	diamond	air	450	2021	64
$SmNiO_3$ films	cBN	air	200	2019	65
KH_2PO_4 (KDP) crystal	diamond	air	160	2021	68
WC-Co (3D printed)	cBN	air	600	2022	74
NiCoCr medium entropy alloy	cBN	air	750	2022	76

References

1. H. Vo et al. Small-Scale Mechanical Testing on Proton Beam-Irradiated 304 SS from Room Temperature to Reactor Operation Temperature, JOM 67 (2015) 2959.
2. B. Bose et al. Temperature dependence of the anisotropic deformation of Zr-2.5%Nb pressure tube material during micro-indentation, J. Nucl. Mater. 419 (2011) 235.
3. M.A. Monclús et al. Optimum high temperature strength of two-dimensional nanocomposites, APL Materials 1 (2013) 052103.
4. M.A. Monclús et al. Microstructure and mechanical properties of physical vapor deposited Cu/W nanoscale multilayers: Influence of layer thickness and temperature, Thin Solid Films 571 (2014) 275.
5. M.A. Monclús et al. Effect of layer thickness on the mechanical behaviour of oxidation-strengthened Zr/Nb nanoscale multilayers, J. Mater. Sci. 53 (2018) 5860.
6. L.W. Yang et al. Mechanical properties of metal-ceramic nanolaminates: effect of constraint and temperature, Acta Mater. 142 (2018) 37.
7. N. Rohbeck et al. In-situ nanoindentation of irradiated silicon carbide in TSIRO particle fuel up to 500 °C, J. Nucl. Mater. 465 (2015) 692.
8. N. Rohbeck et al. Evaluation of the mechanical performance of silicon carbide in TRISO fuel at high temperatures, Nuclear Engineering and Design 306 (2016) 52.
9. D. Frazer et al. High-Temperature Nanoindentation of SiC/SiC Composites, JOM 2019; doi:10.1007/s11837-019-03860-7.
10. Z. Huang et al. Nanoindentation creep study on an ion beam irradiated ODS alloy, J. Nucl. Mater. 451 (2014) 162.
11. Z. Huang et al. A high temperature mechanical study on PH 13-8 maraging steel, Mater. Sci. Eng. A 651 (2016) 574.
12. B.-S. Li et al. Measuring the brittle-to-ductile transition temperature of tungsten–tantalum alloy using chevron-notched micro-cantilevers, Scr. Mater. 180 (2020) 77.
13. J.S.K.-L. Gibson et al. High-temperature indentation of helium-implanted tungsten, Mater. Sci. Eng. A 625 (2015) 38.
14. Y. Zhang et al. High temperature indentation-based property measurements of inconel IN-617, Int. J. Plasticity, 96 (2017) 264.
15. A.J. Harris et al. Extreme nanomechanics: vacuum nanoindentation and nanotribology to 950 ºC, Tribology 9 (2015) 174.
16. A.J. Harris et al. Development of high temperature nanoindentation methodology and its application in the nanoindentation of polycrystalline tungsten in vacuum to 950C, ExpMech 57 (2017) 1115.
17. B.D. Beake et al. Temperature dependence of strain rate sensitivity, indentation size effects and pile-up in polycrystalline tungsten from 25-950 °C, Mater. Design 156 (2018) 278.
18. F. Giuliani et al. Deformation behaviour of TiN and Ti-Al-N coatings at 295 to 573 K, Thin Solid Films 688 (2019) 137363.
19. V. Bhakhri et al. Instrumented nanoindentation investigation into the mechanical behavior of ceramics at moderately elevated temperatures, J. Mater. Res. 27 (2012) 65.
20. G.S. Fox-Rabinovich et al. Impact of mechanical properties measured at room and elevated temperatures on wear resistance of cutting tools with TiAlN and AlCrN coatings, SCT 200 (2006) 5738.
21. G.S. Fox-Rabinovich et al. Impact of annealing on the microstructure, properties, and cutting performance of AlTiN coating, Surf. Coat. Technol. 201 (2006) 3524.
22. G.S. Fox-Rabinovich et al. Effect of annealing below 900°C on structure, properties and tool life of an AlTiN coating under various cutting conditions, Surf. Coat. Technol. 202 (2008) 2985.
23. B.D. Beake et al. Coating optimisation for high-speed machining with advanced nanomechanical test methods, SCT 203 (2009) 1919.
24. B.D. Beake et al. Investigating the correlation between nano-impact fracture resistance and hardness/modulus ratio from nanoindentation at 25-500°C and the fracture resistance and lifetime of cutting tools..., Surf. Coat. Technol. 201 (2007) 4585.

25. B.D. Beake et al. Why can TiAlCrSiYN-based adaptive coatings deliver exceptional performance under extreme frictional conditions? Faraday Discussions 156 (2012) 267.
26. G.S. Fox-Rabinovich et al. Mechanism of adaptability for the nano-structured TiAlCrSiYN-based hard physical vapor deposition coatings under extreme frictional conditions, J. Appl. Phys. 111 (2012) 064306.
27. B.D. Beake et al. Elevated temperature micro-impact testing of TiAlSiN coatings produced by physical vapour deposition, Thin Solid Films 688 (2019) 137358.
28. R. Ctvrtlik et al. Mechanical properties of amorphous silicon carbonitride thin films at elevated temperatures, J. Mater. Sci. 50 (2015) 1553.
29. B.D. Beake et al. Progress in high temperature nanomechanical testing of coatings for optimising their performance in high speed machining, Surf. Coat. Technol. 255 (2014) 102.
30. J.G. Swallow et al. Operando reduction of elastic modulus in (Pr, Ce)O2-□ thin films, Acta Mater. 105 (2016) 16.
31. J. Milhans et al. Mechanical properties of solid oxide fuel cell glass-ceramic seal at high Temperatures, J Power Sources 196 (2011) 5599.
32. A. Sawant et al. High temperature nanoindentation of a Re-bearing single crystal Ni-base superalloy, Scr. Mater. 58 (2008) 275.
33. A. Sawant et al. High temperature nanoindentation of Ni-base superalloys, Superalloys2008, Eds. RC Reed et al, TMS (2008) 863.
34. S.K. Korte et al. High temperature microcompression and nanoindentation in vacuum, J. Mater. Res. 27 (2012) 167.
35. J.S.K.-L. Gibson et al. On extracting mechanical properties from nanoindentation at temperatures up to 1000 °C, Extreme Mechanics Letters 17 (2017) 43.
36. H.N. Mathur et al. Deformation in the □-$Mg_{17}Al_{12}$ phase at 25-278 °C, Acta Mater. 113 (2016) 221.
37. M. Haghshenas et al. Effect of temperature and strain rate on the mechanisms of indentation deformation of magnesium, MRS Comm. 2015. doi:10.1557/mrc.2015.57
38. P. Li et al. Rapid characterization of local shape memory properties through indentation, Sci. Rep 7 (2017) 14827.
39. S. Korte et al. Micropillar compression of ceramics at elevated temperatures, Scr. Mater. 60 (2009) 807.
40. S. Korte et al. Deformation of silicon – insights from micro compression testing at 25–500 °C, Int J Plasticity 27 (2011) 1853.
41. S. Koch et al. A high temperature nanoindentation study of Al-Cu wrought alloy, Mater. Sci. Eng. A 6 (2015) 218.
42. M.-M. Primorac et al. Elevated temperature mechanical properties of novel ultra-fine grained Cu-Nb composites, Mater. Sci. Eng. A 625 (2015) 296.
43. N.M. Everitt et al. High temperature nanoindentation - the importance of isothermal contact, Philos. Mag. 91 (2011) 1221.
44. M. Rebelo de Figueiredo et al. Nanoindentation of chemical-vapor deposited Al_2O_3 hard coatings at elevated temperatures, Thin Solid Films 578 (2015) 20.
45. F. De Luca et al. Nanomechanical Behaviour of Individual Phases in WC-Co Cemented Carbides, from Ambient to High Temperature, Materialia 12 (2020) 100713.
46. D.E.J. Armstrong et al. Bending testing of Silicon Cantilevers from 21°C to 770°C, JOM 67 (2015) 2914.
47. J.S.K.-L. Gibson et al. Mechanical characterisation of the protective Al_2O_3 scale in Cr_2AlC MAX Phases, J.Eur.Ceram.Soc. 39 (2019) 5149.
48. B.D. Beake et al. Nanomechanics to 1000 °C for high temperature mechanical properties of bulk materials and hard coatings, Vacuum 159 (2019) 17.
49. C.H. Bumgardner et al. Probing the local creep mechanisms of SiC/SiC ceramic matrix composites with high-temperature nanoindentation, Journals of Materials Research 36 (2021) 2420-2433.
50. T.J. Marrow et al. High temperature spherical nano-indentation of graphite crystals, Carbon 191 (2022) 236-242.
51. H. Wang et al. Constitutive modelling of a δ-phase zircaloy hydride based on strain rate dependent nanoindentation and nano-scale impact dataset, International Journal of Plasticity 133 (2020) 102787
52. Q. Zhou et al. A nanoindentation study of Ti-based high entropy bulk metallic glasses at elevated temperatures, Journal of Non-Crystalline Solids 532 (2020) 119878
53. Q. Zhou et al. Identifying the high entropy effect on plastic dynamics in bulk metallic glasses: A nanoindentation study at room and elevated temperature, Materials & Design 189 (2020) 108500.
54. H. Wang et al. Nanoindentation based properties of Inconel 718 at elevated temperatures: A comparison of conventional versus additively manufactured samples, International Journal of Plasticity, 120 (2019) 380-394.
55. D. Frazer et al. Elevated temperature nanoindentation creep study of plastically deformed and spark plasma sintered UO_2, Journal of Nuclear Materials 545 (2021) 152605.
56. B. Gong et al. Nano- and-micro-indentation testing of sintered UO_2 fuel pellets with controlled microstructure and stoichiometry, Journal of Nuclear Materials 516 (2019) 169-177.
57. J. Fan et al. High-temperature nanoindentation characterization of sintered nano-copper particles used in high power electronics packaging, Results in Physics 33 (2022) 105168.
58. J. Thornby et al. Micromechanics and indentation creep of magnesium carbon nanotube nanocomposites: 298K-573K, Materials Science and Engineering: A 801 (2021) 140418.
59. X.M. Mei et al. Achieving enhanced mechanical properties of SiC/Al-Cu nanocomposites via simultaneous solid-state alloying of Cu and dispersing of SiC nanoparticles, Materials Science and Engineering: A 860 (2022) 144338.
60. C.M. Rost et al. On the thermal and mechanical properties of $Mg_{0.2}Co_{0.2}Ni_{0.2}Cu_{0.2}Zn_{0.2}O$ across the high-entropy to entropy-stabilized transition, APL Mater 10 (2022) 121108.
61. E. Wyszkowska et al. Investigation of the mechanical properties of ODS steels at high temperatures using nanoindentation technique, Nuclear Instruments and Methods in Physics Research Section B: Beam Interactions with Materials and Atoms 444 (2019) 107-111.
62. C. Tromas et al. Nanoindentation-induced deformation twinning in MAX phase Ti2AlN, Acta Materialia 227 (2022) 117665.
63. R.N. Sarafet al. Investigation and the thermal creep properties of Al/SiC composites made by the powder metallurgy technique, Fourth Canada-Japan Workshop on Composites – CRC Press (2020) 105-114.
64. C.C. Yuan et al. Anelastic and viscoplastic deformation in a Fe-based metallic glass, Journal of Alloys and Compounds 853 (2021) 157233.
65. J. Chen et al. Mechanical and correlated electronic transport properties of preferentially oriented SmNiO3 films, Ceramics International 46 (2020) 6693-6697.
66. E. Bouzakis, Fatigue endurance assessment of DLC coatings on high-speed steels at ambient and elevated temperatures, Coatings 10 (2020) 547.
67. Y. Chen et al. High temperature indentation creep mechanism of metal-ceramic nanolaminates, Mater. Sci. Eng. A 802 (2021).
68. Q. Liu et al. On the improvement of the ductile removal ability of brittle KDP crystals via temperature-effect, Ceram. Int. (2021).
69. Y.-C. Zhang et al. Elastic modulus and hardness characterisation for microregion of Inconel 625/BNi-2 vacuum brazed joint by high temperature indentation, Vacuum 181 (2020) 109582.
70. S. Shen et al. Deformation mechanism and mechanical properties of TiN/ZrN nanolaminates by nanoindentation: effect of layer thickness and temperature, Surf. Coat. Technol. 455 (2022) 129230.
71. T. Polcar et al. High temperature behavior of nanolayered CrAlTiN coating: thermal stability, oxidation and tribological properties, Surf. Coat. Technol. 257 (2014) 70-77.
72. Y. Zhang et al. Visualizing in situ microstructure dependent crack tip stress distribution in IN-617 using nano-mechanical Raman spectroscopy, JOM 68 (2016) 2742-2747.
73. Y. Zhang et al. Visualizing stress and temperature distribution during elevated temperature deformation of IN-617 using nano-mechanical Raman spectroscopy, JOM 70 (2018) 464-468.
74. G. Rui et al. Small-scale mechanical response at intermediate/high temperature of 3D printed WC-Co, Procedia CIRP 108 (2022) 507-512.
75. F. De Luca et al. Nanomechanical response of tungsten carbide single crystals in extreme conditions: Temperature and strain rate dependence, Materialia 27 (2023) 101706.
76. B.B. Zhang et al. Inhibiting creep in nanograined alloys with stable grain boundary networks, Science 378 (2022) 659-663.b